Haar Scale 3 Wavelet Based Investigation Of Fractional Differential Equations

Ratesh Kumar[1],

[1]*School of Chemical Engineering and Physical Sciences*
Lovely Professional University, Punjab

Abstract : The aim of the proposed study is to develop a new hybrid method using Haar scale 3 wavelets for the investigation of fractional Models governed by the Fractional differential equations. Haar scale 3 wavelets are used to estimate the solution by series approximation. To handle the fractional derivatives and integrals in the problems, Caputo sense definition of derivatives and Riemann-Liouville definitions of integrals are used. Numerical solution has been produced for five different fractional differential equations to establish the competency of the proposed method.

Keywords: Haar scale 3 wavelets, Fractional Differential Equations, Caputo derivatives, Quasi-linearization (65L10)

1 Introduction

Fractional calculus is the study of the mathematical science that comes out of the customary meaning of the integer-order differentiation and integration. It gives a few tools for fathoming arbitrary order differential and integral equation. The fractional calculus is as old as traditional calculus, however, has gained significant importance amid the previous few decades, because of its immense importance in various assorted fields of science and engineering which include fluid flow, viscoelasticity, solid mechanics, signal processing, probability, statistics, etc. The number of works managing dynamical frameworks portrayed by fractional-order equation that include derivative and integral of arbitrary order as they delineate the memory and innate properties of various substances. In 1695, L'Hopital wrote a letter to Leibnitz in which he used to get some information about a particular notation he published for derivative of the linear function with order n. He made an inquiry to Leibniz, what may the result be if n is half. Leibniz responded by saying that it is an obvious conundrum, which will result in significant outcomes one day. So, this was the first time when fractional derivative came into the picture.

Fractional calculus emerged as a great tool in explaining the physical and chemical phenomenon with alienate kinetics having microscopic complex behavior. There are fractional differential models which have a non-differentiable but continuous solution such as Weierstrass type functions[1]. These kinds of characteristics are not possible to explain with the help of ordinary or partial differential models. Earlier the field of fractional calculus was purely mathematical without any visible application but in these days, fractional calculus has gained a huge importance because of its application in the various field like theory of thermo-elasticity[2], viscoelastic fluids[3], dynamics of earthquakes[4, 5], fluid dynamics[6, 7], etc. In one of the experiments of Bagley and Torvik in which they studied the motion of rigid plate immersed into the Newtonian fluid. It was found in the experiment that retarding force is proportional to the fractional derivative of the displacement instead of the velocity. It has been observed during the experiment also that fractional model is superior to the integer-order model for the prediction of characteristics of the same material. It has also been observed experimentally and from the real-time observation that there are many complex systems in the real world like relaxation in viscoelastic material, pollution diffusion in the surrounding, charge transport in amorphous semiconductors and many more which show anomalous dynamics. This capability of fractional differential equations in explaining the abnormal dynamic happing in the system with more efficiency and accuracy has gained huge attention from the scientific community. Many of the important classical differential equations with integer-order has got extensions to the generalized fraction differential equation with an arbitrary order for in-depth study of the corresponding physical model

But general closed-form solution for fractional differential equation has yet not been established. Therefore, many researchers are involved in developing the various numerical and semi-analytic schemes for investigating the different phenomena governed by the fractional equation such as Adomian decomposition method [8], , Haar wavelet method with dilation factor 2[9] , Homotopy analysis method[8], Generalized Taylor collocation method [10] , Variational iteration method[7] Fractional iteration method[11] , Bessel collocation method [12] , Chebyshev wavelet method [13] , Fractional Taylor Method[14], Hybrid functions approximation [15] , Gegenbauer Wavelet Method[16], Reproducing kernel [17], Sumudu transformation method [18] etc.

But the study of characteristics of different materials governed by these fractional differential equations has yet not been investigated by Haar scale 3 wavelet-based technique. Wavelets are one of the modernistic orthonormal functions which have a capability of dilation and translation. Because of these properties, numerical techniques which involve wavelets bases are showing the qualitative improvement in contrast with other methods. In literature, dyadic wavelets are in preponderance. In 1995, Chui and Lian [19] has developed the Haar scale 3wavelets by using the process of multiresolution analysis. In 2018, Mittal and Pandit have used the Haar scale 3wavelets [20-22] for solving the various types of differential equations and found that these wavelet bases are equally competent in solving the various types of mathematical models governed by differential equations. Also, it was shown by them that the Haar scale 3wavelet has a faster rate of convergence as compared to the dyadic wavelets. Moreover, investigation of characteristics of different phenomena governed by fractional differential equation has yet not been much studied by Haar scale 3 wavelet methods. This encourages us to develop a new technique using Haar scale 3 for analyzing the behavior of systems governed by these fractional differential equations [23-24].

The prime purpose of proposed work is to establish a new computational technique for obtaining the solution of fractional equations emerging in the various field of science and technology using Haar scale 3 wavelet bases.

This chapter follows the sequence of sections as described: In section 2, the basic definitions of fractional calculus are given. In section 3, explicit forms of Haar scale 3 parent wavelets with their families and procedure to find their integrals have been explained briefly. Representation of the solution using Haar scale 3 wavelets is explained in section 4. Section 5 explains the method of solution using Haar scale 3wavelets. In section 6, Argument for the convergence of the technique is given. In section 7, solutions of five different examples of fractional differential equations are produced using the present method to analyze the efficiency and performance of the present method. In section 8, the conclusion drawn from the results and in future research idea is given.

2 Some basic definitions of Fractional calculus

2.1 Mittag-Leffler Function

It is an extension of exponential function which has huge importance in the field of fractional calculus. It has two forms of expression as given below

i. ***One Parameter Mittag-Leffler Function*** [23]for a set of complex numbers and any positive real no α is defined as

$$E_{\alpha} = \sum_{m=0}^{\infty} \frac{z^m}{\Gamma(\alpha m+1)} \; , \alpha > 0, \alpha \epsilon \mathbb{R} \; , z \in \mathbb{C} \tag{2.1}$$

ii. ***Two-Parameter Mittag-Leffler Function*** [23] for a set of complex numbers and for positive real no's α , β is defined as

$$E_{\alpha,\beta} = \sum_{m=0}^{\infty} \frac{z^m}{\Gamma(\alpha m+\beta)} \; , \alpha , \beta > 0, \alpha, \beta \epsilon \mathbb{R}, z \in \mathbb{C} \tag{2.2}$$

2.2 Riemann-Liouville Fractional Integral Operator [23]

The fractional integral operator defined by the mathematician Riemann-Liouville for the positive real nos. α , a, t over the interval $[a, b]$ is given by

$${}_{RL}J_a^{\alpha} f(t) = \frac{1}{\Gamma(\alpha)} \int_a^t f(z)(t-z)^{\alpha-1} dz \tag{2.3}$$

where α denotes the order of derivative and $t \epsilon [a, b]$.

2.3 Riemann-Liouville Fractional Differential Operator [23]

The fractional differential operator defined by the mathematician Riemann-Liouville for the positive real nos. α , a, t over the interval $[a, b]$ is given by

$${}_{RL}D_a^{\alpha} f(t) = \begin{cases} \frac{1}{\Gamma(m-\alpha)} \frac{d^m}{dt^m} \int_a^t \frac{f(z)}{(t-z)^{\alpha-m+1}} dz \; , m-1 < \alpha < m \in \mathbb{N} \\ \frac{d^m}{dt^m} f(t) \qquad , \qquad \alpha = m \in \mathbb{N} \end{cases} \tag{2.4}$$

where α denotes the order of derivative and $t \epsilon [a, b]$.

2.4 Caputo Fractional Differential Operator [23]

The fractional differential operator defined by the Italian mathematician Caputo for the positive real nos. α , a, t is

$${}_{C}D_a^{\alpha} f(t) = \begin{cases} \frac{1}{\Gamma(m-\alpha)} \int_a^t \frac{f^m(z)}{(t-z)^{\alpha-m+1}} dz \; , m-1 < \alpha < m \in \mathbb{N} \\ \frac{d^m}{dt^m} f(t) \qquad , \qquad \alpha = m \in \mathbb{N} \end{cases} \tag{2.5}$$

where α denotes the order of derivative and $t \epsilon [a, b]$.

3 Integrals of Haar scale 3 Wavelet

The closed-form expressions for father wavelet, symmetric and antisymmetric mother wavelets for Haar scale 3 wavelet family [19], [25-27] are given below

Haar scale 3 function

$$\varphi(t) = \begin{cases} 1 & 0 \le t < 1 \\ 0 & elsewhere \end{cases} \tag{3.1}$$

Haar scale 3 symmetric wavelet function

$$\psi_1(t) = \frac{1}{\sqrt{2}}\begin{cases} -1 & 0 \le t < \frac{1}{3} \\ 2 & \frac{1}{3} \le t < \frac{2}{3} \\ -1 & \frac{2}{3} \le t < 1 \\ 0 & elsewhere \end{cases} \tag{3.2}$$

Haar scale 3 antisymmetric wavelet function

$$\psi_2(t) = \sqrt{\frac{3}{2}}\begin{cases} 1 & 0 \le t < \frac{1}{3} \\ 0 & \frac{1}{3} \le t < \frac{2}{3} \\ -1 & \frac{2}{3} \le t < 1 \\ 0 & elsewhere \end{cases} \tag{3.3}$$

The main difference which makes the Haar scale 3wavelets better than the dyadic wavelets is that only one mother wavelet is responsible for the construction of whole wavelet family but in case of Haar scale 3wavelets, two mother wavelets with different shapes are responsible for the construction of the whole family. Because of this fact, Haar scale 3 wavelets increase the convergence rate of the solution. Wavelets represented by equations (3.2)-(3.3) are the mother wavelets which generate the whole Haar scale 3wavelet family. A multi-resolution analysis is used to get the whole Haar scale 3 wavelet family as defined below.

3.1 Multi-resolution Analysis (MRA)

MRA for the space $L_2(R)$ is demarcated as a sequence of subspace $W_j, V_j \subset L_2(R), j \in \mathbb{Z}$ which closed and has the features as given below

$a)\ \phi(t) \in V_0 \ \Rightarrow \phi(3^j t) \in V_j$

$b)\ \phi(t) \in V_0 \ \Rightarrow \varphi(3^j t - k) \in V_j$

$c)\ \psi^i(t) \in W_0^i, i = 1,2 \ \Rightarrow \psi^i(3^j t) \in W_j^i$

$d)\ \psi^i(t) \in W_0^i, i = 1,2 \ \Rightarrow \psi^i(3^j t - k) \in W_j^i$

$e)\ W_J = W_j^1 \oplus W_j^2 = \oplus W_j^i \ , i = 1,2$

$f)\ \cdots \subset V_0 \subset V_1 \subset V_2 \subset V_3 \subset V_4 \subset \cdots$

$g)\ \cdots \perp W_0 \perp W_1 \perp W_2 \perp W_3 \perp W_4 \perp \cdots$

$h)\ V_j = V_0 + \sum_{i=0}^{j-1} W_j^1 + \sum_{i=0}^{j-1} W_j^2$

$i)\ \phi(t) \in V_0\ implies\ \phi(\mathrm{t}-\mathrm{k}) \in V_0; k \in \mathbb{Z}$ and it forms Riesz basis in V_0

Now using the above said propertied, comprehensive explicit form of Haar scale 3 wavelet family is obtained as:

$For\ \ i=1$

$$h_i(t)=\varphi(t)=\begin{cases}1 & 0\le t<1\\ 0 & elsewhere\end{cases} \tag{3.4}$$

$For\ \ \ i=2,4,\dots 3p-1$

$$h_i(t)=\psi^1\left(3^j t-k\right)=\frac{1}{\sqrt{2}}\begin{cases}-1 & \alpha_1(i)\le t<\alpha_2(i)\\ 2 & \alpha_2(i)\le t<\alpha_3(i)\\ -1 & \alpha_3(i)\le t<\alpha_4(i)\\ 0 & elsewhere\end{cases} \tag{3.5}$$

$For\ \ \ i=3,6,\dots 3p$

$$h_i(t)=\psi^2\left(3^j t-k\right)=\sqrt{\frac{3}{2}}\begin{cases}1 & \alpha_1(i)\le t<\alpha_2(i)\\ 0 & \alpha_2(i)\le t<\alpha_3(i)\\ -1 & \alpha_3(i)\le t<\alpha_4(i)\\ 0 & elsewhere\end{cases}, \tag{3.6}$$

where $\alpha_1(i)=\frac{k}{p},\alpha_2(i)=\frac{3k+1}{3p},\ \alpha_3(i)=\frac{(3k+2)}{3p},\ \alpha_4(i)=\frac{k+1}{p},\ p=3^j\ ,\ j=0,1,2,\dots,\ k=0,1,2,\dots,p-1.$

Here $i\,,j\,,k$ respectively represent the wavelet number, level of resolution (dilation) and translation parameters of wavelets family. The values of $i\ (for\ i>1)$ can be calculated with help of $j\,,k$ by using the following relations $\begin{Bmatrix}i-1=3^j+2k & for\ even\ i\\ i-2=3^j+2k & for\ odd\ i\end{Bmatrix}$.By using this relation for different dilation and translations of $h_2(t),h_3(t)$, we will get the wavelet family as $h_2(t),h_3(t),h_4(t),h_5(t),h_6(t),\dots$ where $h_2(t)$ and $h_3(t)$ are also called mother wavelets and rest all the wavelets which we have obtained from mother wavelet are called daughter wavelets.

Now one can easily integrate the equations (3.4)-(3.6) the desired number of times over the interval [A, B) by using Riemann Liouville Integral formula [23] as given below

$$q_{\beta,i}(t)=\frac{1}{\Gamma(\beta)}\int_A^t h_i(x)(t-x)^{\beta-1}dx\qquad\forall\quad 0\le\beta\le m\,,\qquad m=1,2,3\dots\dots\ ,\qquad i=1,2,3,\dots\dots 3p \tag{3.7}$$

Appling the definition as given in Equation (3.7) on Equations (3.4) -(3.6), we get

$$q_{\beta,i}(t)=\frac{t^\beta}{\Gamma(\beta+1)}\qquad for\ \ i=1 \tag{3.8}$$

$q_{\beta,i}(t)'s\ \ for\ \ i=2,4,6,8,\cdots,3p-1$ are given below

$$q_{\beta,i}(t)=$$

$$\frac{1}{\sqrt{2}}\begin{cases}0 & for\quad 0\le\ t\le\alpha_1(i)\\ \frac{-1}{\Gamma(\beta+1)}\left(t-\alpha_1(i)\right)^\beta & for\ \ \alpha_1(i)\le t\le\alpha_2(i)\\ \frac{1}{\Gamma(\beta+1)}\left[-\left(t-\alpha_1(i)\right)^\beta+3\left(t-\alpha_2(i)\right)^\beta\right] & for\ \ \alpha_2(i)\le t\le\alpha_3(i)\\ \frac{1}{\Gamma(\beta+1)}\left[-\left(t-\alpha_1(i)\right)^\beta+3\left(t-\alpha_2(i)\right)^\beta-3\left(t-\alpha_3(i)\right)^\beta\right] & for\ \alpha_3(i)\le t\le\alpha_4(i)\\ \frac{1}{\Gamma(\beta+1)}\left[-\left(t-\alpha_1(i)\right)^\beta+3\left(t-\alpha_2(i)\right)^\beta-3\left(t-\alpha_3(i)\right)^\beta+\left(t-\alpha_4(i)\right)^\beta\right] & for\ \alpha_4(i)\le t\le 1\end{cases} \tag{3.9}$$

$q_{\beta,i}(t)'s\ \ for\ \ i=3,5,7,9,\cdots,3p$ are given by

$$q_{\beta,i}(t)=$$

$$\sqrt{\frac{3}{2}}\begin{cases} 0 & for \quad 0 \le t \le \alpha_1(i) \\ \frac{1}{\Gamma(\beta+1)}\left(t-\alpha_1(i)\right)^{\beta} & for \quad \alpha_1(i) \le t \le \alpha_2(i) \\ \frac{1}{\Gamma(\beta+1)}\left[\left(t-\alpha_1(i)\right)^{\beta}-\left(t-\alpha_2(i)\right)^{\beta}\right] & for \quad \alpha_2(i) \le t \le \alpha_3(i) \\ \frac{1}{\Gamma(\beta+1)}\left[\left(t-\alpha_1(i)\right)^{\beta}-\left(t-\alpha_2(i)\right)^{\beta}-\left(t-\alpha_3(i)\right)^{\beta}\right] & for \quad \alpha_3(i) \le t \le \alpha_4(i) \\ \frac{1}{\Gamma(\beta+1)}\left[\left(t-\alpha_1(i)\right)^{\beta}-\left(t-\alpha_2(i)\right)^{\beta}-\left(t-\alpha_3(i)\right)^{\beta}+\left(t-\alpha_4(i)\right)^{\beta}\right] & for \, \alpha_4(i) \le t \le 1 \end{cases} \tag{3.10}$$

4 Approximation of solution

Using the properties of Haar scale 3 wavelets as explained in section 3, any function $x(t) \in L_2(R)$ can be represented by the infinite Haar series as

$$x(t) = \sum_{i=0}^{\infty} a_i h_i(t) = a_1 h_1(t) + \sum_{even\ i} a_i \psi^1\left(3^j t - k\right) + \sum_{odd\ i>1} a_i \psi^2\left(3^j t - k\right) \tag{4.1}$$

Here $a_i's$ are the wavelet coefficients and their values are to be determined by the proposed method. But for the computational purpose, one has to consider a finite number of terms. By considering the first $3p$ terms to approximate the function $u(t)$ we get

$x(t) \approx u_{3p} = \sum_{i=0}^{3p} a_i h_i(t)$ where $p = 3^j, j = 0,1,2, ...$ (4.2)

5 Method of Solution based on Haar scale 3 wavelets

Consider the following Fractional DE(differential equation)

$\alpha D^2 x(t) + \beta D^{\alpha_1} x(t) + \gamma D^{\alpha_2} x(t) + \delta x(t) = g(t)$ (5.1)

with initial conditions $x(0) = \delta_2$, $x'(0) = \delta_3$, where α , β, γ, δ are the arbitrary constants and $1 < \alpha_1 < 2$,$0 < \alpha_2 < 1$

Now the solution x(t) for the above equation can be obtained using the following steps α_2

Step1: Approximate $D^2 x(t)$ (derivative of biggest order) using the Haar scale 3 wavelet bases as

$$D^2 x(t) = \sum_{i=0}^{3p} a_i h_i(t) = a_1 h_1(t) + \sum_{even\ i} a_i \psi^1\left(3^j t - k\right) + \sum_{odd\ i>1} a_i \psi^2\left(3^j t - k\right) \tag{5.2}$$

where $a_i' s$ for i=0,1, 2…,3p are the nondyadic wavelet coefficients

Step 2: By integrating the equation (5.2) within the limits 0 to t, we get

$x'(t) = \sum_{i=0}^{3p} a_i q_{1,i}(t) + y'(0) = \sum_{i=0}^{3p} a_i q_{1,i}(t) + \delta_3$ (5.3)

Again, integrating the equation (5.3) within the limits 0 to t, we get

$x(t) = \sum_{i=0}^{3p} a_i q_{2,i}(t) + \delta_3 t + y(0) = \sum_{i=0}^{3p} a_i q_{2,i}(t) + \delta_3 t + \delta_2$ (5.4)

Step 3: Differentiate the equation (5.4) using Caputo definition of fractional derivatives we get

$$D^{\alpha_1} x(t) = \sum_{i=0}^{3p} a_i q_{2-\alpha_1,i}(t) + \delta_3 \frac{1}{\Gamma(2-\alpha_1)} (t)^{1-\alpha_1} \tag{5.5}$$

$D^{\alpha_2} x(t) = \sum_{i=0}^{3p} a_i q_{2-\alpha_2,i}(t) + \delta_3 \frac{1}{\Gamma(2-\alpha_2)} (t)^{1-\alpha_2}$ (5.6)

Step 4: Using equations (5.2)-(5.6),Equation (5.1) becomes

$$\alpha \sum_{i=0}^{3p} a_i h_i(t) + \beta \left[\sum_{i=0}^{3p} a_i q_{2-\alpha_1,i}(t) + \delta_3 \frac{1}{\Gamma(2-\alpha_1)} (t)^{1-\alpha_1} \right] + \gamma \left[\sum_{i=0}^{3p} a_i q_{2-\alpha_2,i}(t) + \delta_3 \frac{1}{\Gamma(2-\alpha_2)} (t)^{1-\alpha_2} \right] + \delta [\sum_{i=0}^{3p} a_i q_{2,i}(t) + \delta_3 t + \delta_2] = g(t) \tag{5.7}$$

After simplification, we get

$$\sum_{i=0}^{3p} a_i [\alpha h_i(t) + \beta q_{2-\alpha_1,i}(t) + \gamma\, q_{2-\alpha_2,i}(t) + \delta q_{2,i}(t)] = g(t) - \left[\beta \delta_3 \frac{1}{\Gamma(2-\alpha_1)} (t)^{1-\alpha_1} + \gamma \delta_3 \frac{1}{\Gamma(2-\alpha_2)} + \delta(\delta_3 t + \delta_2) \right] \tag{5.8}$$

Step 4: After Discretizing the equation (5.8) using the collocation points we get the following matrix system

$$aH = F \tag{5.9}$$

Then using the Thomas algorithm, we obtained the wavelet coefficients $a_i's$. Then by substituting the values of wavelet coefficients $a_i's$ in equation (5.4), we get the Haar scale 3 wavelet-based solution of Fractional differential equations with the given initial conditions. Similarly, by using the above steps we can generate the solution for boundary conditions.

6 Convergence analysis

Mittal and Pandit [24] has proved that if $x(t)\, \epsilon L^2(R)$ such that $|x^m(t)| \leq M, \forall\, t\epsilon(0,1)$ where M is any real constant and x(t) is approximated by Non-dyadic(Scale 3) Haar wavelet family as given below:

$$x_{3p}(t) = \sum_{i=0}^{3p} a_i h_i(t) \tag{6.1}$$

Then the error bound for the solution $x(t)$ using L_2-norm is calculated as

$$\|x(t) - x_{3p}(t)\| \leq \left(\frac{2}{3}\right)^{2(m-\alpha)} \frac{8\, M^2}{\left(\Gamma(m-\alpha+1)\right)^2} \left(\frac{3^{-2(j+1)(m-\alpha+1)}}{1 - 3^{-2(m-\alpha)+1}} \right) \tag{6.2}$$

which ensures the convergence of approximated solution with the increase in value of j. Moreover, for exact values of m, α and M, then the maximum value of error bound can also be calculated.

7 Error Analysis by Numerical Experiments

To describe the appropriateness of the proposed technique for the Fractional differential equations of fractional order, solutions of five different problems obtained by the proposed computational technique have been analysed. Also, the efficiency of the present scheme is tested by calculating the error with the help of following formula

$$\text{Absolute error} = |x_{exact}(t_l) - x_{num}(t_l)| \tag{7.1}$$

where t_l's are the collocation points.

Experiment No. 1: $D^2x + D^{\frac{3}{2}}x + x = t^2 + 4\sqrt{\frac{t}{\pi}} + 2$ under the boundary constraints $x(0) = 0, x(1) = 1$ (7.2)

Analytic solution of the problem is $x(t) = t^2$

After applying the method of solution discussed in section 5 the following solution is proposed

$$x(t) = \sum_{i=1}^{3p} a_i[q_{2,i}(t) - tq_{2,i}(1)] + t \tag{7.3}$$

$a_i's$ are the wavelets coefficients which will be obtained by the following procedure and $q_{j,i}'s$ are the wavelets integrals which have been already calculated in section 3.After applying the proposed scheme on Equation (7.2), it reduced to the following system

$$\sum_{i=0}^{3p} a_i\left[\sqrt{\pi t}\left(h_i(t) + q_{\frac{1}{2},i}(t) + q_{2,i}(t)\right) - \left(\sqrt{\pi}t^{\frac{3}{2}} + 1\right)q_{2,i}(1)\right] = 4t + 1 + \sqrt{\pi}\left[t^{\frac{5}{2}} - t^{\frac{3}{2}} + 2t^{\frac{1}{2}}\right] \tag{7.4}$$

After discretizing the equation(7.4) using the collocation points we get the following matrix system $aH = F$

After solving the above matrix, we fatch the values of $a_i's$.which will be used to find out the solution. Results achieved by the proposed technique are conferred by the graphs and tables for the better visibility of accuracy. Figure 7.1 and Table 7.1 demonstrate the clearly visible agreement in the exact and approximated solutions. In Table 7.2 results attained by the proposed algorithm are compared with other method existing in the recent literature and found it outperform over others methods like VIM[7], HAM[8], Reproducing Kernel Analysis (RKA)[17] ,which demonstrates the superiority and reliability of the method. Figure 7.2 is depicting the high level of accuracy (which is of order 10^{17}) obtained at the different collocation points.

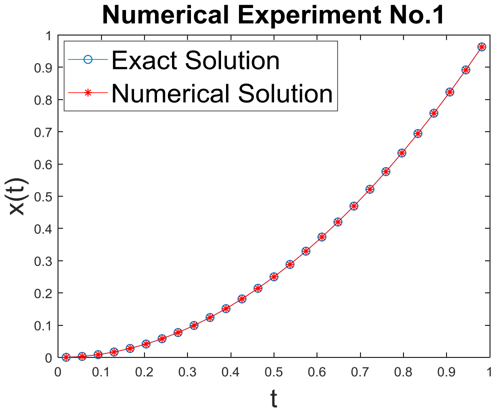

Figure 7.1: Comparison of exact and numerical solution of Numerical experiment No.1 at J=2

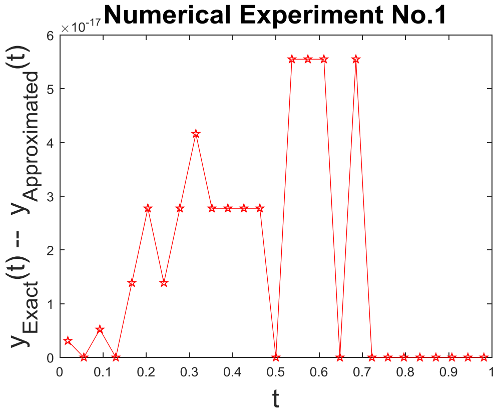

Figure 7.2: Absolute error at the different collocation points considered for the solution of experiment No.1

Numerical Experiment No. 2: $D^2x(t) + 0.5\,D^{\frac{1}{2}}x(t) + x(t) = 3 + t^2\left(\frac{1}{\Gamma(2.5)}t^{-0.5} + 1\right)$ w.r.t B. C's $x(0) = 0\,, x(1) = 2$ (7.5)

Analytic solution of Equation (7.5) is $x(t) = t^2 + 1$. After applying the technique of solution discussed in the section 5 the following solution is proposed

$$x(t) = \sum_{i=1}^{3p} a_i[q_{2,i}(t) - tq_{2,i}(1)] + t + 1 \tag{7.6}$$

$a_i's$ are the wavelets coefficients which will be obtained by the following procedure and $q_{j,i}'s$ are the wavelets integrals which has been already calculated in section 3.

After applying the proposed technique on the equation no.(7.5). It reduced to the following system

$$\sum_{i=0}^{3p} a_i \left[\left(h_i(t) + \frac{1}{2} q_{\frac{3}{2},i}(t) + q_{2,i}(t) \right) - \left(\frac{t^{\frac{1}{2}}}{\sqrt{\pi}} + t \right) q_{2,i}(1) \right] = t^2 - t + 2 + \left[\frac{4}{3\sqrt{\pi}} t^{\frac{3}{2}} - \frac{1}{\sqrt{\pi}} t^{\frac{1}{2}} \right] \quad (7.7)$$

After discretizing the equation (7.7) using the collocation points we get the matrix system

$$aH = F$$

After solving the above matrix system, we get the vales of $a_i's$.which will be used to find out the solution. It can be observed from the
Table 7.1 and Figure 7.3 that the results achived agrees well with analytic solution, which demostrate high efficiency of the proposed tecnique to solve these kinds of problems.Also from Table 7.2, we can conclude that proposed technique is a strong solver in terms of better accuracy in comparison with the other method [17] . Figure 7.4 is showing the errors at the different colocation points.

Table 7.1: Comparision of results achieved with other methods for Experiment. No.1

t	**Analytic**	**Haar Scale 3 Solution**	**Present Method(E*)**	**RKA(E*)**[17]	**VIM(E*)**[7]	**HAM(E*)**[8]
0.1	0.01	0.0100000000000000	6.93889390390723e-18	0	0.5487432e−4	2.3265e-13
0.2	0.04	0.0400000000000000	0	0	0.6312556e−3	1.4385e-11
0.3	0.09	0.0900000000000000	0	0	0.2665571e−2	6.1890e-11
0.4	0.16	0.1600000000000000	2.77555756156289e-17	0	0.7480121e−2	2.2736e-11
0.5	0.25	0.2500000000000000	0	2.77555756156289e-17	0.1679592e−1	1.3680e-10
0.6	0.36	0.3600000000000000	0	5.55111512312578e-17	0.3277307e−1	3.5678e-11
0.7	0.49	0.4900000000000000	5.55111512312578e-17	5.55111512312578e-17	0.5806535e−1	2.6188e-10
0.8	0.64	0.6400000000000000	0	1.11022302545678e-17	0.9588508e−1	4.3416e-10
0.9	0.81	0.8100000000000000	0	1.11022302545678e-17	0.1500768448	1.0816e-10

E*(Absolute Error)

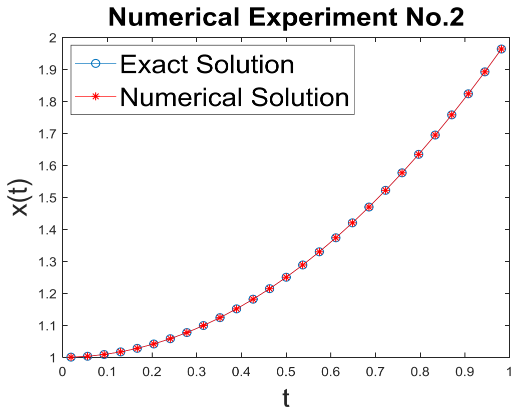

Figure 7.3: Comparison of exact and numerical solution of experiment No.2 at J=2

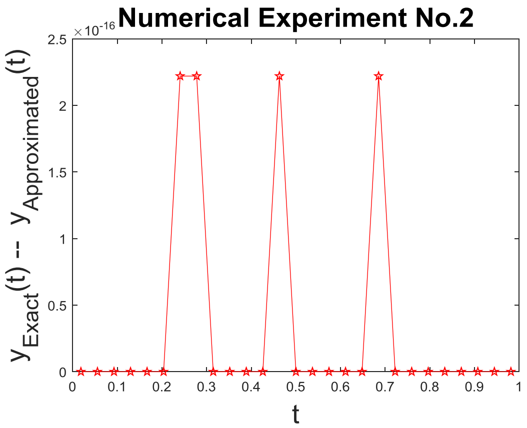

Figure 7.4: Absolute error in the solution of experiment No.2 at the collocation points

Table 7.2: Comparison of results attained with other methods for Experiment. No.2

t	**Analytic solution**	**Haar Scale 3 Solution**	**Present Method(E*)**	**RKA(E*)**[17]
0.1	1.01	1.0100000000000000000	0	1.932676241e-
0.2	1.04	1.0400000000000000000	0	3.161981788e-
0.3	1.09	1.0900000000000000000	0	3.679907490e-
0.4	1.16	1.1600000000000000000	0	3.661697390e-
0.5	1.25	1.2500000000000000000	0	3.300057339e-
0.6	1.36	1.3600000000000000000	0	2.745960126e-
0.7	1.49	1.4900000000000000022204	2.22044604925031e-	2.096272045e-
0.8	1.64	1.6400000000000000000	0	1.404942829e-
0.9	1.81	1.8100000000000000000	0	7.004619107e-

E* (Absolute Error)

Numerical Experiment No. 3:Consider the equation $D^2x(t) + D^{\frac{1}{2}}x(t) + x(t) = 2 + t^2\left(\frac{2}{\Gamma(2.5)}t^{-0.5} + 1\right) - t\left(\frac{1}{\Gamma(1.5)}t^{-0.5} + 1\right)$ subjected to the boundary condition $x(0) = 0\,, x(1) = 0$

Analytic solution of Equation (7.8) (7.8)

is $x(t) = t^2 - t$ .After applying the proposed method following solution is obtained

$$x(t) = \sum_{i=1}^{3p} a_i[q_{2,i}(t) - tq_{2,i}(1)] \quad (7.9)$$

$a_i's$ are the wavelets coefficients which will be obtained by the procedure discussed above and $q_{j,i}'s$ are the wavelets integrals which has been already calculated in section 3.

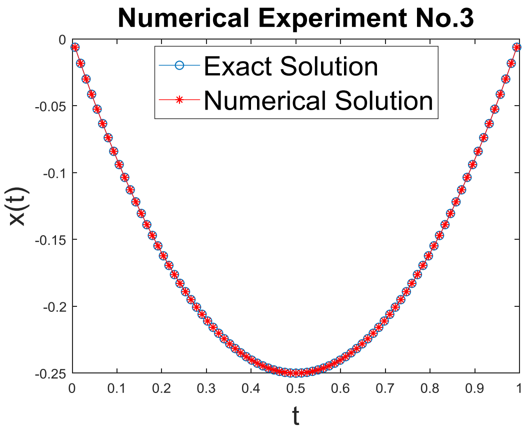

Figure 7.5: Comparison of exact and numerical solution of experiment No.3 at J=2

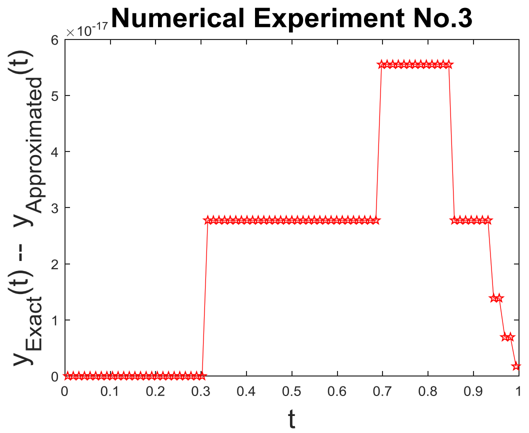

Figure 7.6: Absolute error in the solution of experiment No.3 at different collocation pts.

Table 7.3: Comparision of results achived with other methods for Experiment. No.3

t	**Analytic**	**Haar Scale 3 Solution**	**Present Method (E^*)**	**RKA(E^*)**[17]
0.	-	-	0	4.178019042e
0.	-	-	-	6.892891813e
0.	-	-	5.55111512312578e	8.052572498e
0.	-	-	5.55111512312578e	8.010652391e
0.	-	-	5.55111512312578e	7.193844853e
0.	-	-	5.55111512312578e	5.949374826e
0.	-	-	5.55111512312578e	4.504783491e
0.	-	-	2.77555756156289e	2.989430925e
0.	-	-	2.77555756156289e	1.473612898e

E^* (Absolute Error)

Table 7.3 depicting the performance of the method in contrast with other method existing in the recent literature. It validates the high efficiency and performance of the method. Getting high accuracy for a small number of grid points makes it strong solver for these kinds of mathematical models. Figure 7.5 demonstrates that the results achieved with the proposed technique agree well with exact solution and Figure 7.6 explains the errors in the solution at the different collocation points.

Numerical Experiment No. 4: $D^2x(t) + D^{\frac{3}{2}}x(t) + x(t) = t + \frac{1}{\sqrt{\pi t}} + 1$ subjected to the boundary condition $x(0) = 0\,,\ x'(1) = 1$ (7.10)

Analytic solution of the problem is $x(t) = t + 1$

By using the method of solution discussed in the section 3, we proposed the following solution for the above equations

$$x(t) = \sum_{i=1}^{3p} a_i q_{2,i}(t) + t + 1 \tag{7.11}$$

$a_i{'s}$ are the wavelets coefficients which will be obtained by the procedure discussed above and $q_{j,i}{'s}$ are the wavelets integrals which has been already calculated in section 3. It is shown in Table 7.4 and Figure 7.8 that results achived with the proposed tecnique exactly mathcing with exact solution with no error.It is also shown in the Table 7.4 that the results achived with the proposed tecnique are superior than the results obtained by the other methods availabe in the existing litrature. Figure 7.7 explains the high level of agreement bethween the exact and Haar Scale 3 Solution.

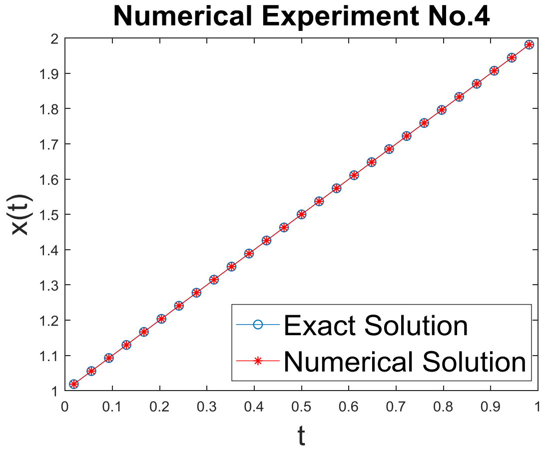

Figure 7.7: Comparison of exact and numerical solution of experiment No.4 at J=2

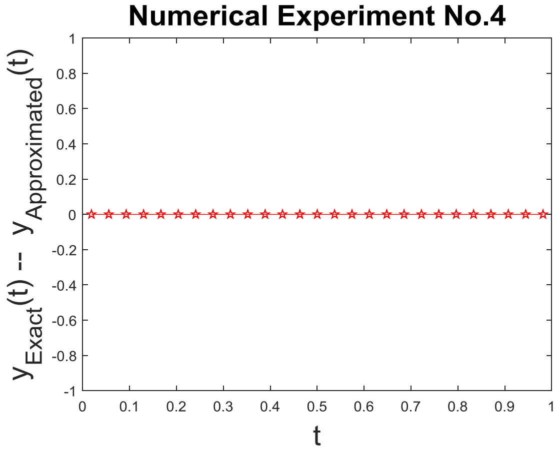

Figure 7.8: Absolute error in the solution of experiment No.4 at different collocation pts

Table 7.4: Comparison of results achieved with other methods in the existing literature for Experiment. No.4

t	**Analytic solution**	**Haar Scale 3 Solution**	**Present Method (E^*)**	**RKA(E^*)**[17]	**BCM(E^*)**[12]
0.1	1.1	1.1	0	0	9.3742e-16
0.2	1.2	1.2	0	0	3.9634e-15
0.3	1.3	1.3	0	0	4.2834e-15
0.4	1.4	1.4	0	0	3.2975e-15
0.5	1.5	1.5	0	0	2.0455e-15
0.6	1.6	1.6	0	2.220446049E-	1.0277e-15
0.7	1.7	1.7	0	0	3.4773e-16
0.8	1.8	1.8	0	0	6.9289e-17
0.9	1.9	1.9	0	2.220446049E-	2.3947e-16

E^* (Absolute Error)

8 Conclusion

After looking at the results of five numerical experiments performed with proposed technique, we infer that differential equation of fractional order can easily be solved by the proposed scheme with less computational cost and high accuracy. For example, in numerical experiment no. 1 level of accuracy obtained is or order 10^{-17} for only 9 colocation points in the first iteration. Moreover, the use of common MATLAB subprograms to solve various types of fractions equations, makes it more computer friendly. Very good accuracy is obtained for a very small number of collocation points and the results achieved are better than or at par with the other methods existing in the recent literature. It makes the proposed scheme a strong solver for these kinds of fractional differential equations. Therefore, by looking at the performance of the method, we conclude that the given method can be extended to solve other set of fractional differential equations. All the calculations have been performed using the MATLAB 7.

8.1 References

[1]. Zahle, M., & Ziezold, H. (1996). Fractional derivatives of Weierstrass-type functions. *Journal of Computational and Applied Mathematics*, **76**(1996), 265–275.

[2]. Povstenko, Y.Z. (2009). Thermoelasticity that uses fractional heat conduction equation. *Journal of Mathematical Sciences*, **162**(2), 296–305. https://doi.org/10.1007/s10958-009-9636-3

[3]. Tripathi, D., Pandey, S.K., & Das, S. (2010). Peristaltic flow of viscoelastic fluid with fractional Maxwell model through a channel. *Applied Mathematics and Computation*, **215**(10), 3645–3654. https://doi.org/10.1016/j.amc.2009.11.002

[4]. Lopes, A.M., Tenreiro Machado, J.A., Pinto, C.M. A., & Galhano, A.M.S.F. (2013). Fractional dynamics and MDS visualization of earthquake phenomena. *Computers and Mathematics with Applications*, **66**(5), 647–658. https://doi.org/10.1016/j.camwa.2013.02.003

[5]. Momani, S., & Odibat, Z. (2006). Analytical approach to linear fractional partial differential equations arising in fluid mechanics. Physics Letters, Section A: General. *Atomic and Solid State Physics*, **355**(4–5), 271–279. https://doi.org/10.1016/j.physleta.2006.02.048

[6] Mukherjee, R. (2020). Electrical, thermal and elastic properties of methylammonium lead bromide single crystal. Bulletin of Materials Science, *43*(1), 1-5.

[7]. Ray, S.S., & Bera, R.K. (2005). Analytical solution of the Bagley Torvik equation by Adomian decomposition method. *Applied Mathematics and Computation*, **168**(1), 398–410. https://doi.org/10.1016/j.amc.2004.09.006

[8] Mukherjee, R., Lawes, G., & Nadgorny, B. (2014). Enhancement of high dielectric permittivity in CaCu3Ti4O12/RuO2 composites in the vicinity of the percolation threshold. Applied Physics Letters, *105*(7), 072901.

[9]. Ghorbani, A., & Alavi, A. (2008). Application of He's variational iteration method to solve semi differential equations of n th order. *Mathematical Problems in Engineering*, 2008, 1–9. https://doi.org/10.1155/2008/627983

[10] Mukherjee, R., Huang, Z. F., & Nadgorny, B. (2014). Multiple percolation tunneling staircase in metal-semiconductor nanoparticle composites. Applied Physics Letters, *105*(17), 173104.

[11]. Fadravi, H. H., Nik, H. Saber., & R. Buzhabadi. (2011). Homotopy Analysis Method Based on Optimal Value of the Convergence Control Parameter for Solving Semi-Differential Equations. *Journal of Mathematical Extension*, **5**(2), 105–121.

[12]. Çenesiz, Y., Keskin, Y., & Kurnaz, A. (2010). The solution of the Bagley-Torvik equation with the generalized Taylor collocation method. *Journal of the Franklin Institute*, **347**(2), 452–466. https://doi.org/10.1016/j.jfranklin.2009.10.007

[13]. Saha Ray, S. (2012). On Haar wavelet operational matrix of general order and its application for the numerical solution of fractional Bagley Torvik equation. *Applied Mathematics and Computation*, **218**(9), 5239–5248. https://doi.org/10.1016/j.amc.2011.11.007

[14]. Mekkaoui, T., & Hammouch, Z. (2012). Approximate analytical solutions to the Bagley-Torvik equation by the fractional iteration method. *Annals of the University of Craiova, Mathematics and Computer Science Series*, **39**(2), 251–256.
[15]. Yuzbasi, S. (2013). Numerical solution of the Bagley-Torvik equation by the Bessel collocation method. *Mathematical Methods in the Applied Sciences*, **36**(3), 300–312. https://doi.org/10.1002/mma.2588
[16]. Mohammadi, F. (2014). Numerical solution of Bagley-Torvik equation using Chebyshev wavelet operational matrix of fractional derivative MSC : *International Journal of Advances in Applied Mathematics and Mechanics*, **2**(1), 83–91.
[17]. Krishnasamy, V.S., & Razzaghi, M. (2016). The Numerical Solution of the Bagley–Torvik Equation With Fractional Taylor Method. *Journal of Computational and Nonlinear Dynamics*, **11**(5), 051010. https://doi.org/10.1115/1.4032390
[18]. Mashayekhi, S., & Razzaghi, M. (2016). Numerical solution of the fractional Bagley-Torvik equation by using hybrid functions approximation. *Mathematical Methods in the Applied Sciences*, **39**(3), 353–365. https://doi.org/10.1002/mma.3486
[19]. Srivastava, H.M., Shah, F.A., & Abass, R. (2019). An Application of the Gegenbauer Wavelet Method for the Numerical Solution of the Fractional Bagley-Torvik Equation. *Russian Journal of Mathematical Physics*, **26**(1), 77–93. https://doi.org/10.1134/S1061920819010096.
[20]. Abu Arqub, O., & Maayah, B. (2018). Solutions of Bagley–Torvik and Painlevé equations of fractional order using iterative reproducing kernel algorithm with error estimates. *Neural Computing and Applications*, **29**(5), 1465–1479. https://doi.org/10.1007/s00521-016-2484-4
[21]. Jena, R. M., & Chakraverty, S. (2019). Analytical solution of Bagley-Torvik equations using Sumudu transformation method. *SN Applied Sciences*, **1**(3), 1–6. https://doi.org/10.1007/s42452-019-0259-0
[22]. Chui, C.K., & Lian, J.A. (1995). Construction of Compactly Supported Symmetric and Antisymmetric Orthonormal Wavelets with Scale 3. *Applied and Computational Harmonic Analysis*, **2**(1), 21–51
[23]. Mittal, R. C., & Pandit, S. (2018b). Quasilinearized Scale-3 Haar wavelets-based algorithm for numerical simulation of fractional dynamical systems. *Engineering Computations*, **35**(5), 1907–1931. https://doi.org/https:// doi.org/10.1108/EC-09-2017-0347.
[24]. Mittal, R. C., & Pandit, S. (2018). New Scale-3 Haar Wavelets Algorithm for Numerical Simulation of Second Order Ordinary Differential Equations. Proceedings of the National Academy of Sciences, India Section A: Physical Sciences, (ii). https://doi.org/https://doi.org/10.1007/s40010-018-0538-y
[25]. Mittal, R.C., & Pandit, S. (2017). Sensitivity analysis of shock wave Burgers' equation via a novel algorithm based on scale-3 Haar wavelets. *International Journal of Computer Mathematics*, (March), 1–25. https://doi.org/10.1080/00207160.2017.1293820
[26]. Das, S. (2011). Functional Fractional Calculus. In Functional Fractional Calculus (second). https://doi.org/10.1007/978-3-642-20545-3
[27]. Mittal, R. C., & Pandit, S. (2018c). Quasilinearized Scale-3 Haar wavelets-based algorithm for numerical simulation of fractional dynamical systems. *Engineering Computations (Swansea,*